

## STRUCTURE IDENTIFICATION OF METAL FIBRE REINFORCED CEMENTITIOUS COMPOSITES

JIŘÍ VALA \*

**Abstract.** Mechanical properties of metal fibre reinforced cementitious composites, because of the danger of micro- and macro-cracking due to the mechanism of quasi-brittle fracture, depend strongly on the macrostructural homogeneity and directional distribution of fibres. Thus some low-invasive or quite non-destructive measurement techniques, together with non-expensive, quick, robust and reliable algorithms for evaluation of corresponding material parameters, are needed. This paper demonstrates some promising classes of such approaches, based on image processing and indirect magnetic and electromagnetic measurements, with the aim of the development of general methodology for technical evaluation of such materials.

**Key words.** Composite materials, non-destructive testing, computational homogenization, inverse problems, image processing.

**AMS subject classifications.** 35R30, 35Q61, 74Q05, 68U10.

**1. Introduction.** Advanced building structures frequently use materials as silicate composites, reinforced by metal particles, preventing the tension stresses and strains as sources of undesirable micro- and macro-cracking; the most frequently used material of this type is the steel fibre reinforced concrete. However, mechanical behaviour of such composites is determined by the choice of fibre properties and their volume fraction, location and orientation in the matrix, sensitive to the technological procedures (as special compaction) and to the early-age treatment – cf. [29], [13] and [25]. The employment of the destructive approach relies usually on the separation of particles, taken from the early-age matrix, alternatively obtained from the crushed part of the existing structure, in the laboratory; consequently the volume fraction of particles can be evaluated accurately, whereas any information related to the original orientation of particles is missing. Moreover, such experiments with many structures are not allowed by technical standards. Thus the employment of non- or (at least) semi-destructive measurement methods, applicable in situ, handling homogeneity and isotropy, as well as the volume fraction of fibres, is required.

A reasonable tool for testing of internal material structures without their damage is offered by radiographic methods, combined with the image processing analysis; for its advantages and limitations (namely for the difficulties in non-invasive testing of massive structures) see [12], [9], [10] and [36], for the 3-dimensional computer tomography cf. [18] and [38]. Several alternative methods have been presented in the literature: [35] estimates the effective material permittivity employing a coaxial probe together with microwave reflectometry techniques, [22] comes from the AC-impedance spectroscopy, [15] performs special low-frequency electrical resistance measurements, [7] develops a method based on impedance-over-frequency measurements, employing certain two-electrode probe, supported by the numerical fast Fourier transform, and [6] and [39] make use of the ferromagnetic behaviour of metal particles to evaluate their volume fraction, whereas the deviation of values obtained from measurements then gives basic information concerning the required homogeneity and isotropy.

---

\*Institute of Mathematics and Descriptive Geometry, Faculty of Civil Engineering, Brno University of Technology, 60200 Brno, Veverří 331/95, Czech Republic (vala.j@fce.vutbr.cz).

In general, reliable prediction of mechanical, thermal, etc. behaviour of composites, including (rather small) fibres incorporated into a matrix, can be also performed using electromagnetic measurements, combined with computational simulation of the corresponding physical process and solution of inverse problems of identification of selected material parameters by [11]. This approach needs distinguishable values of material characteristics, namely of electrical permittivity or magnetic permeability, which is true e.g. for metal particles in concrete, glass or ceramic matrices.

The special experimental configuration usually tries to force a (nearly) stationary process, whose mathematical description works with a differential operator close to the classical Laplace one, to enable non-expensive software simulation. Consequently, the crucial problem is to implement a correct evaluation procedure for an effective relative permeability (or permittivity, etc.) using the incomplete data on the material microstructure and on relative permeability of particular components; a generalization to more than two components is possible. Simple linear formulas, supplied by heuristic recommendations, generate the results far from those observed in practice. For spherical particles the classical Maxwell-Garnett mixing formula is available; by [28] this can be interpreted as a (very rough) estimate of effective permittivity, whose improvement leads to the new (much more complicated) explicit formula, based on the approximation of a cylindrical particle with a rotational ellipsoid with the dominant main axis. Such generalization by [8] comes from the so-called Brugemann approach and the repeated usage of similar ellipsoids as reference volume elements.

Various geometrical simplifications, incorporated in the homogenization techniques, frequently supported by physical arguments, lead to rather different results. In the Maxwell-Garnett mixing rule, namely with spherical particles, [16] admits the presence of multiple scattering, important for high volume fractions of fibres. No additional physical assumptions are needed, again for periodic spheres, in [14]: the auxiliary problem, referring to the mathematical theory of homogenization of elliptic operators, can be then analyzed (including the existence and uniqueness of solution, the convergence of sequences of approximate solutions, etc.) using the two-scale convergence theorems (or, alternatively, similar results from the asymptotic analysis,  $G$ -convergence,  $H$ -convergence,  $\Gamma$ -convergence, etc.) by [3] and [17]; the crucial (seemingly) explicit formula for the evaluation of an effective parameter value, comes from the method of oscillating test functions by [32]. The corresponding theory of finite element discretization is developed in [5]. Some modifications for periodic structures with cubes and cylinders (instead of spheres) are introduced in [21]. In [40] the difficulties with complex particle shapes are handled using the boundary integral approach thanks to the knowledge of general solutions of the Laplace equation, with Heaviside characteristic functions of particles. Unfortunately, further generalization of this approach (namely to non-periodic structure, avoiding all mixing tricks), sketched in [24], cannot avoid serious (partially still open) problems of mathematical analysis, namely to the convergence using probability measures by [31] or abstract (a priori deterministic) homogenization structures related to  $\sigma$ -convergence by [19].

Computational analysis of more complicated physical, chemical etc. processes, namely those active on certain microscale, hidden from the macroscopic point of view, able to be detected only from indirect observations, perhaps partially from some mesoscale analysis, have typically to be done separately, a posteriori applying some statistical methods (Voronoi tessellations, reverse Monte Carlo optimization), least square optimization, etc. The dissipative particle dynamics, referring up to the atomistic or molecular scale, adopted to handle certain super-particles, results in [30]

in the discrete element method. Unlike such formulation, in [4] and [2] the micromechanical computational model for the description of the macroscopic behaviour of such a class of materials, composed by a matrix phase and a fibre reinforcing phase, is formulated; the macro-constitutive equations of unidirectional or randomly distributed fibre reinforced materials are then obtained by taking into account the possibility of crack formation and propagation in the matrix, of fibre debonding and breaking.

This paper follows the research priorities of the project AdMaS UP at FCE BUT (for more information see *Acknowledgments*). According to the limited extent of the paper, we shall sketch the computational algorithms, working with the data sets obtained from the most important experimental techniques, with the final aim to compose certain general methodology for the identification of crucial material parameters for mechanical, thermal, etc. properties of metal fibre reinforced cementitious composites, with numerous references to the literature containing technical details (including existence, convergence, sensitivity and reliability considerations) and practical applications. We shall pay attention (using i), ii) for the future references) namely

- i) to the volume of fraction of metal fibres,
- ii) to the distribution of directions of metal fibres,

not to the detailed structure of a hardened cementitious part containing sand grains fixed in a cementitious binder, or to the cohesion between such matrix and fibres.

**2. Image processing techniques.** The best choice for identification of i) and ii) should be (if possible) a direct method, classifiable as a non-destructive or low-invasive one, without any requirements to deeper physical analysis. This seems to be satisfied by image processing techniques. As two such representative techniques, let us present the exploitation of 2-dimensional radiographic images and of 3-dimensional tomographic ones.

**2.1. 2-dimensional radiographic images.** The radiographic method has been developed and applied by [9] for a rather large class of building materials. It comes from the gray-scale planar images and their post-processing modifications. Finally all fibres are reduced to one-pixel thin curves whose direction classes can be detected and corresponding histograms drawn. However, using the two-dimensional fast Fourier transform, following [33] (with the straightforward application to textile textures), most artificial modifications can be avoided. For simplicity, let  $f(x, y)$  be the grey level at pixel coordinates, related to a square image containing  $N \times N$  pixels. Then the direct and inverse Fourier transforms are

$$F(u, v) = \sum_{x,y=0}^{N-1} f(x, y) \exp \frac{-2\pi i(ux + vy)}{N}, \quad f(x, y) = \frac{1}{N^2} \sum_{u,v=0}^{N-1} F(u, v) \exp \frac{2\pi i(ux + vy)}{N}$$

and finally the power spectrum  $P(u, v) = |F(u, v)|^2$  contains all needed information for our (more reader-friendly) evaluations. This can be identified with a special diffraction process where both sums for  $N \rightarrow \infty$  are converted to integrals – cf. [36].

Figure 2.1 presents an example of derivation of the histogram of directions using the two-dimensional discrete Fourier transform: the planar image comes from the standard X-ray 160 kV apparatus, 8 characteristic directions related to classes of angles of the same size  $\pi/8$  are emphasized to demonstrate the potential anisotropy of a fibre concrete sample. Principal advantages and drawbacks of this approach are evident just from this simple example. The numerical treatment, based on the fast Fourier transform using the original code in MATLAB, is rather simple and inexpensive. The macroscopic material anisotropy, unwelcome in this case, is evident immediately: the worst reinforced class of directions contains only 48% of fibres in

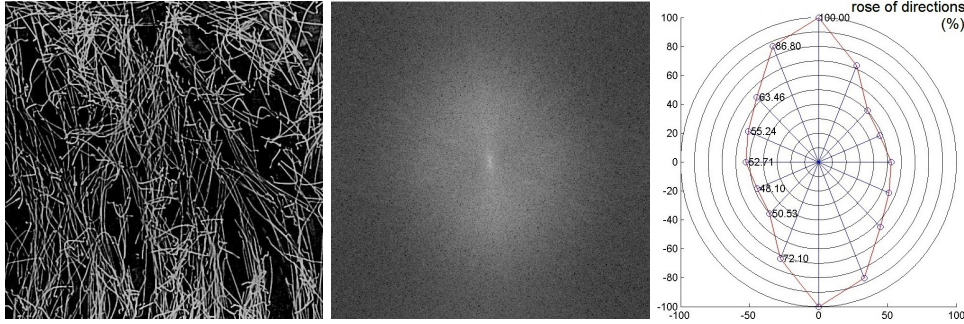


FIG. 2.1. Example of planar radiographic image (left photo). Power spectrum (central image). Distribution ("rose") of fibre directions (right graph).

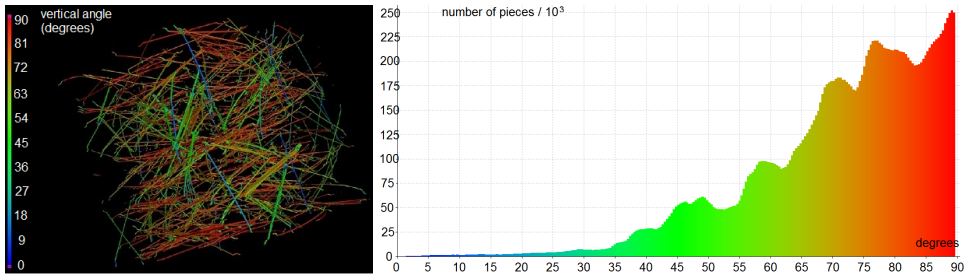


FIG. 2.2. Example of 3-dimensional tomographic image (left photo). Corresponding cumulative distribution of fibre directions (right graph).

comparison with the best one. Such analysis can be repeated several times due to particular cuts through the specimen; nevertheless, material composition far from the building surface (without its destruction) are nearly invisible. The reliable evaluation of i) (see the last paragraph in *Introduction*) from a low number of planar images is also not available.

**2.2. 3-dimensional tomographic images.** Some unpleasant properties of the image processing exploiting the planar radiographic images can be overcome using appropriate industrial tomographs. The tomograph *GE Phoenix v|tome|x L 300* has been recently installed in the Centre AdMaS at FCE BUT (cf. the project AdMaS UP in *Acknowledgements*); however, Figure 2.1 refers to the (rather expensive) screening using the tomograph *GE Phoenix v|tome|x L 240* including its software image processing support, installed in CEITEC (Central European Institute of Technology, Brno University of Technology in collaboration with Masaryk University in Brno).

Spatial distributions of fibre directions on (2.1) are only illustrative. However, the detailed description of the position of all particular fibres is available for prescribed types of cubic and cylindrical material specimens. These data can be very useful for the validation of other approaches, namely of the electromagnetic ones (cf. the following section), coupled with Monte Carlo (or similar) simulations or with some kind of (usually periodic) homogenization. In particular, the influence of the system error coming from the violation of the assumption of negligible small fibres should be analyzed carefully. The left and central parts of Figure 2.1 show an example of such numerical evaluation, exploiting the standard ANSYS software, corresponding to the magnetic approach, introduced in the subsection 3.1. The rest of Figure 2.1 demonstrates a possibility of Monte Carlo generation of non-penetrating fibre positions even in the case of high volume fraction of fibres, using the original MATLAB software by [23].

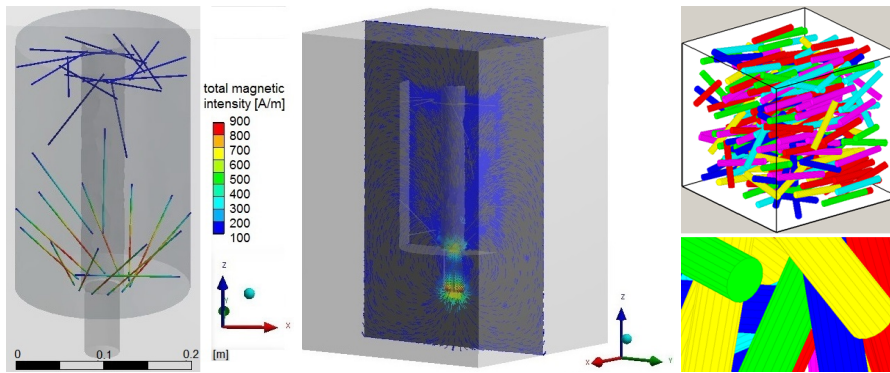


FIG. 2.3. Example of numerical simulation of the stationary magnetic field total intensity in the composite structure, detected from the 3-dimensional tomographic image, applied to the cylindrical specimen: in particular fibres (left figure) and in the whole measurement system corresponding to Figure 3.1 (central figure). Example of Monte Carlo generation of the composite material structure containing non-penetrating fibres with prescribed shapes, directional distribution and volume fraction and its typical detail (right scheme).

**3. Electromagnetic approaches.** As evident from the discussion of image processing techniques, the development of some alternative indirect techniques is useful. Up to now, the most successful indirect measurement approaches seem to be based on measurements of some magnetic or electromagnetic quantities. However, this requires more proper analysis of physical processes active during the measurement and their similarity to those connected with the deformation and fracture of composites.

**3.1. Physical and mathematical background.** Up to now, the most successful indirect measurement approaches seem to be based on measurements of some magnetic or electromagnetic quantities, All magnetic or electromagnetic approaches make use of the different values of such measurable effective time-independent material characteristics as the dielectric permittivity  $\varepsilon$ , the electric conductivity  $\sigma$ , and the magnetic permeability  $\mu$ , sometimes also of the magnetic susceptibility  $\chi$ . These characteristics can be considered as constant just for (macroscopically) homogeneous materials and as scalar for isotropic ones, which brings technical difficulties namely to the identification of ii). For the sake of brevity we shall assume constant characteristics, in some considerations just scalar (not matrix) ones; however, the form of all relations enables us to come to more complicated cases naturally.

The theory of existence of solution of the complete evolutionary system of Maxwell equations, even of the direct one (i. e. for the a priori known material characteristics), contains still open questions – cf. the “mysteriously difficult problem” by [26], p. 257. This brings obstacles to all proofs of convergence of sequences of approximate solutions, hidden in computational algorithms, as discussed in [1] and [27]. Consequently all reasonable electromagnetic experiments must be based on the very special physical and geometrical setting. In this paper we shall sketch another original methodology, based on the measurements of complex impedance, which seems (both theoretically and from first practical experiments) to be able to cover both i) and ii) naturally.

The analysis of electromagnetic fields works with a set of scalar and vector quantities, introduced on  $\Omega \times I$  where  $\Omega$  is a domain in the 3-dimensional Euclidean space, supplied by Cartesian coordinates, and  $I$  means a finite time interval; dots refer to partial time derivatives. Using the notation of [20], pp. 1 and 4, such basic quantities on  $\Omega \times I$  are the scalar real volume charge density  $\rho$  and the following 3-dimensional real vectors: the electric current density (charge flux)  $J$ , the electric field intensity

$E$ , the magnetic field intensity  $H$ , the electric flux density (electric displacement)  $D$ , the magnetic flux density (magnetic induction)  $B$ , and the magnetization (average magnetic moment per unit volume)  $M$ .

The obvious charge conservation principle, two Gauss laws for electric and magnetic fields and the Ampère and the Faraday laws are

$$(3.1) \quad \dot{\rho} + \nabla \cdot J = 0, \quad \nabla \cdot D = \rho, \quad \nabla \cdot B = 0, \quad \dot{D} - \nabla \times H + J = 0, \quad \dot{B} + \nabla \times E = 0.$$

Following [20], p. 11, we are allowed to consider the linear constitutive equations

$$(3.2) \quad J = \sigma E, \quad D = \varepsilon E, \quad B = \mu H, \quad M = \chi H.$$

Moreover, we can introduce the energy density  $w = \frac{1}{2}(D \cdot E + B \cdot H)$  and the total energy flux (Poynting vector)  $P = E \times H$ ; then we receive, in addition to (3.1),

$$(3.3) \quad \begin{aligned} \dot{w} + \nabla \cdot P + J \cdot E &= \dot{D} \cdot E + \dot{B} \cdot H + \nabla \cdot (E \times H) + J \cdot E \\ &= \dot{D} \cdot E + \dot{B} \cdot H + H \cdot \nabla \times E - E \cdot \nabla \times H + J \cdot E \\ &= (\dot{D} - \nabla \times H + J) \cdot E + (\dot{B} + \nabla \times E) \cdot H = 0, \end{aligned}$$

which can be seen as the energy conservation principle. In addition to (3.3), from (3.1) for homogeneous materials (with zero derivatives of  $\varepsilon$ ,  $\sigma$  and  $\mu$ ) we obtain

$$(3.4) \quad \begin{aligned} \nabla \times \nabla \times H &= \nabla J + \nabla \dot{D} = \sigma \nabla \times E + \varepsilon \nabla \times \dot{E} = -\sigma \dot{B} - \varepsilon \ddot{B} = -\sigma \mu \dot{H} - \varepsilon \mu \ddot{H}, \\ \nabla \times \nabla \times E &= -\nabla \times \dot{B} = -\mu \nabla \times \dot{H} = -\mu \dot{J} - \mu \ddot{D} = -\mu \sigma \dot{E} - \mu \varepsilon \ddot{E}. \end{aligned}$$

Applying the mathematical formula  $\nabla \times \nabla \times S = \nabla(\nabla S) - \nabla \cdot \nabla S$ , for the choice both  $S = H$  and  $S = E$  its left side degenerates, thanks to (3.2), to  $\Delta S = \nabla \cdot \nabla S$ , and (3.4) gets the simple form

$$(3.5) \quad \Delta H = \sigma \mu \dot{H} + \varepsilon \mu \ddot{H}, \quad \Delta E = \mu \sigma \dot{E} - \mu \varepsilon \ddot{E}.$$

A more complicated form of (3.5) and (3.4) can be derived in the same way without any homogeneity assumption. In particular, for isotropic materials  $\varepsilon$ ,  $\sigma$  and  $\mu$  can be considered as scalar constants, thus  $\sigma \mu = \mu \sigma$  and  $\varepsilon \mu = \mu \varepsilon$ .

Especially for the stationary pure magnetic field the second equation and the right side of the first one in (3.5) vanish, which results in the homogeneous Laplace equation  $\Delta H = 0$  with no explicit  $\mu$  (which comes back from the boundary condition). Then the interface boundary condition of type  $(S - S^\times) \cdot \nu = 0$ , with  $S^\times$  in the role of some vector variable  $S$  coming from a domain adjacent to  $S$  (or from external environment) where  $\nu$  is the local (formally outward) unit normal vector to the boundary of  $\Omega$ , can be implemented. This configuration with the natural choice  $S = B$  contains  $\mu$ , thus enables us to exploit some rather simple semi-implicit identification formulae, at least those obtained from the mixture theory by [8]; for more detailed discussion see [36]. Moreover, it seems to be reasonable, analogously to [34], to convert more complicated problems to some similar semi-stationary form, as will be demonstrated here for the special case of harmonic time dependence.

Through the inverse Fourier transform, general solutions of Maxwell equations can be built, following [20], p. 13, as linear combinations of single-frequency solutions

$$(3.6) \quad S(r, t) = \frac{1}{2\pi} \int_{-\infty}^{\infty} \tilde{S}(r, \omega) \exp(-i\omega t) d\omega$$

with  $S \in \{J, E, H, D, B, M\}$  where  $r$  denotes the distance from some selected fixed point from  $\Omega$  in  $R^3$  and the time  $t$  is transformed to the frequency  $\omega$  between 0 and  $2\pi$ ; the phasor amplitudes  $\tilde{S}$  are complex-valued. Consequently, using the notation \* for complex conjugates, we receive  $w = \frac{1}{2} \text{Re}(\tilde{D} \cdot \tilde{E}^* + \tilde{B} \cdot \tilde{H}^*)$  and (3.1) yields

$$(3.7) \quad \nabla \times \tilde{H} = \tilde{J} - i\omega \tilde{D}, \quad \nabla \times \tilde{E} = i\omega \tilde{B}, \quad \nabla \cdot \tilde{D} = \tilde{\rho}, \quad \nabla \cdot \tilde{B} = 0$$

with  $\tilde{\rho}$  introduced similarly to (3.6). Let us remark that (3.7) can be derived even without (3.6), for particular values of  $\omega$ . In addition to (3.7), under the same assumptions on material characteristics, using the identity matrix  $I$ , then (3.5) reads

$$(3.8) \quad \Delta \tilde{H} + \left( I + \sigma \varepsilon^{-1} \frac{i}{\omega} \right) \omega^2 \varepsilon \mu \tilde{H} = 0, \quad \Delta \tilde{E} + \omega^2 \mu \varepsilon \left( I + \varepsilon^{-1} \sigma \frac{i}{\omega} \right) \tilde{E} = 0,$$

which are two separated complex Helmholtz equations (instead of the original real Laplace one), with a (seemingly free) real parameter  $\omega$ .

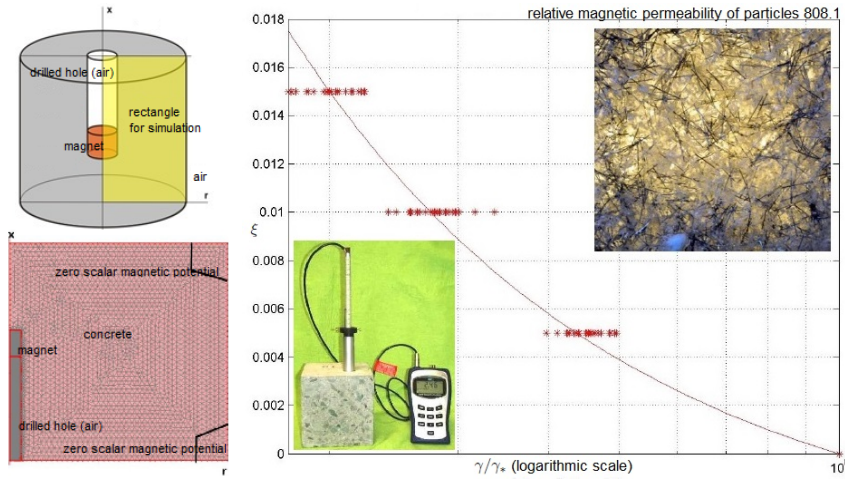


FIG. 3.1. Geometrical configuration of the experiment and its possible computational simplification (left scheme), not needed in Figure 2.1. Evaluation of volume fraction of fibres from Hall probe based measurements (right graph, including photos of the whole measurement equipment with the Hall probe and of the reference epoxy specimen).

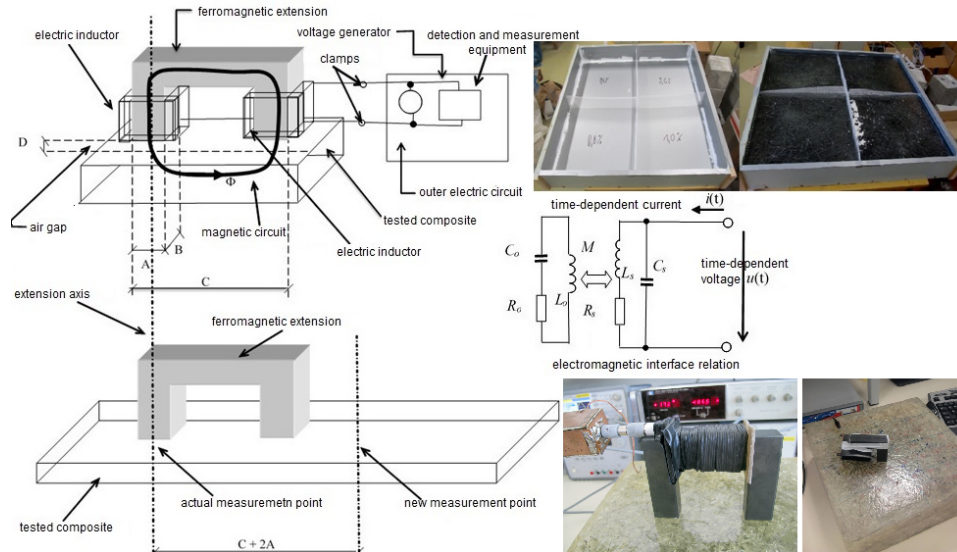


FIG. 3.2. Sketch of the experimental device (left scheme). Idealized one-dimensional model of LRC-circuit (right scheme). Preparation of reference specimens for testing (right upper photos). First experimental equipment for measurements in situ (right lower photos).

**3.2. Stationary magnetic fields.** The generation of (nearly) stationary magnetic field can use certain set of permanent magnets and the Hall probe (based on the

physical Hall effect), whose application can be seen from the left part of Figure 3.1: measured boundary values  $\gamma = B \cdot \nu$ , containing the effective composite permeability  $\mu$ , for certain positive volume fraction of  $\xi$  (unlike the right part of Figure 2.1: 3 sets of transparent specimens with  $\xi \in \{0.5, 1.0, 1.5\}$  are used here) are related to corresponding values  $\gamma_*$  corresponding  $\xi = 0$ ; for more details (including the justification using finite and infinite element modelling in MATLAB and COMSOL) see [36].

Thanks to the expected macroscopic homogeneity and isotropy and the low volume fraction of fibres, the explicit evaluation formula

$$\xi(\mu, \mu_s) = 1 - \frac{\mu_s - \mu}{\mu_s - \mu_c} \left( \frac{\mu_c}{\mu_s} \right)^{3L(1-2L)(2-3L)} \left( \frac{(1+3L)\mu_c + (2-3L)\mu_s}{(1+3L)\mu + (2-3L)\mu_s} \right)^{\frac{(3L-1)^2}{(2-3L)(1+3L)}}$$

where  $\mu_s$  refers to the permeability of steel fibres (not guaranteed by the producer unfortunately),  $\mu_c$  to the known permeability of the remaining material,  $\mu$  to the effective mixture permeability (a priori unknown) in sense of [40] and

$$L = \frac{\zeta}{4\vartheta^3} \left( 2\zeta\vartheta + \ln \frac{\zeta - \vartheta}{\zeta + \vartheta} \right)$$

contains certain shape parameters  $\vartheta$  and  $\zeta$ . As derived in [37], these parameters are just  $\zeta = a/b$  and  $\vartheta = \sqrt{\zeta^2 - 1}$  for all fibres considered as identical rotational ellipsoids with the lengths of main and remaining axes  $a$  and  $b$ .

Some couples  $(\xi, \gamma/\gamma_*)$  from the Hall probe measurements are available for the successful least squares identification of  $\xi$  from any values  $\gamma/\gamma_*$ , as discussed in [36]. However, for higher volume fractions the mutual influence of particular fibres as magnetic dipoles should not be neglected (as in standard mixture theories); for (nearly) periodic structures this can be handled using e. g. the two-scale homogenization, referring to the numerical analysis of certain auxiliary periodic boundary value problem, applied to one partial differential cell equation by [3], p. 96.

In practice, for the identification of  $\xi$  the above sketched magnetic approach can be reliable; nevertheless, this needs to install the Hall probe inside certain number of drilled holes, which allows detection of material structure even inside massive building constructions, but may not be classified as a low-invasive treatment. Moreover, the estimate of fibre orientation is more complicated and practical results may be worse than those from radiographic images.

**3.3. Time-harmonic electromagnetic fields.** The electromagnetic measurement and identification system relies on the analysis coming from (3.8), making use of some special choices and simplifications. In the case for one-dimensional modelling, open to various generalizations, a circuit consisting of (parallel or serial) capacitors, solenoids and resistors can be characterized by their capacitance  $C$ , inductance  $L$  and resistance  $R$ , as sketched on the small right scheme on Figure 3.1, that are proportional to  $\varepsilon$ ,  $\mu$  and  $\sigma$  (in our general notation). Thus, unlike the magnetic approach, more free parameters, including the frequency  $\omega$ , can be utilized, in the formulation of the identification problem, which offers namely a possibility to handle material structures in various distances from the building surface.

The original measurement equipment, designed and constructed at BUT, is now in the process of patent registration, thus the left part of Figure 3.1 shows only the physical idea, not all technical details. Two photos document the preparation of special specimens for calibration curves (which can be correlated with the results of numerical analysis of certain simplified version of (3.8) with homogenized characteristics) and the first experience with practical measurements. However, this method is still in progress, involving the more detailed study of its fundamentals and applicability.

**4. Conclusion.** In this paper we have introduced four methods of experimental identification of i) and ii) and sketched the corresponding computational algorithms. To reach the aim to formulate some general methodology (as promised in *Introduction*), a lot of research work is needed: not only the progress in the mathematical analysis and computational algorithms related i) and ii), including the homogenization effects (formulation of macroscopic material characteristics), but also in the optimization of experimental settings, namely in the case of electromagnetic measurements, and in the proper analysis of similarity of relevant physical processes, needed for any reasonable calibration. New ideas may come from the discussion at *Algoritmy 2016*.

**Acknowledgments.** This paper has been worked out under the project LO1408 *AdMaS UP – Advanced Materials, Structures and Technologies*, supported by Ministry of Education, Youth and Sports of the Czech Republic under the *National Sustainability Programme I*. The author thanks to Prof. L. Hobst, head of the Institute of Building Testing at FCE BUT and the division of AdMaS UP, and his Ph.D. students P. Bílek and T. Komárková for collaboration in experimental material research, to Prof. P. Fiala from the Institute of Microelectronics at FEEC BUT, responsible to nondestructive measurement techniques, to Dr. V. Kozák from the Institute of Physics of Materials AS CR in Brno for intensive discussion on mechanisms of quasi-brittle fracture in composites and to Dr. T. Pospíšil for software support and development.

## REFERENCES

- [1] T. Z. BOULMEZAOUD AND M. EL RHABI, *On time-harmonic Maxwell's equations in Lipschitz and multiply-connected domains of  $R^3$* . Monografias del Seminario Matemático García de Galdeano, 27 (2003), pp. 127–134.
- [2] A. CERRONE, P. WAWRZYNEK, A. NONN, G. H. PAULINO AND A. INGRAFFEA, *Implementation and verification of the Park-Paulino-Roesler cohesive zone model in 3D*. Engineering Fracture Mechanics, 120 (2014), pp. 6–42.
- [3] D. CIORANESCU AND P. DONATO, *An Introduction to Homogenization*. Oxford University, 1999.
- [4] V. M. C. F. CUNHA, J. A. O. BARROS AND J. M. SENA-CRUZ, *An integrated approach for modelling the tensile behaviour of steel fibre reinforced self-compacting concrete*. Cement and Concrete Research, 41 (2011), pp. 64–76.
- [5] Y. EFENDIEV AND T. Y. HOU, *Multiscale Finite Element Methods*. Springer, 2009.
- [6] M. FAIFER, L. FERRARA, R. OTTOBONI AND S. TOSCANI, *Low frequency electrical and magnetic methods for non-destructive analysis of fiber dispersion in fiber reinforced cementitious composites: an overview*. Sensors, 13 (2013), pp. 1300–1318.
- [7] M. FAIFER, R. OTTOBONI, S. TOSCANI AND L. FERRARA, *Nondestructive testing of steel-fiber-reinforced concrete using a magnetic approach*. IEEE Transactions on Instrumentation and Measurement, 60 (2011), pp. 1709–1711.
- [8] S. GIORDANO, *Effective medium theory for dielectric ellipsoids*. Journal of Electrostatics, 58 (2003), pp. 59–76.
- [9] L. HOBST, O. ANTON, J. VODIČKA AND J. ŠČUČKA, *Homogeneity detection of fibre-concrete structures by using radiographic technique*. In: Nondestructive Testing of Materials and Structures, Springer 2013, pp. 323–328.
- [10] L. HOBST AND P. BÍLEK, *Various control methods developed for fibre concrete structures*. Recent advances in integrity, reliability and failure – 4-th International Conference in Funchal (Madeira), 2013, pp. 721-730.
- [11] V. ISAKOV, *Inverse Problems for Partial Differential Equations*. Springer, 2006.
- [12] S. KÄRKKÄINEN AND E. B. VEDEL JENSEN, *Estimation of fibre orientation from digital images*. Image Analysis and Stereology, 20 (2001), pp. 199–202.
- [13] A. KRASNIKOVS, V. ZAHAREVSKIS, O. KONONOVA, V. LUSI, A. GALUSHCHAK AND E. ZALESKIS, *Fiber concrete properties control by fibers motion – investigation in fresh concrete during casting*. Industrial Engineering – 8th International DAAAM Baltic Conference in Tallin, 2012, Part V: Materials Engineering, #10, 6 pp.
- [14] G. KRISTENSSON, *Homogenization of spherical inclusions*. Progress in Electromagnetic Research, 42 (2003), pp. 1–25.
- [15] J. F. LATASTE, M. BEHLOUL AND D. BREYSSE, *Characterisation of fibres distribution in a steel fibre reinforced concrete with electrical resistivity measurements*. NDT & E International (Independent Nondestructive Testing and Evaluation), 41 (2008), pp. 638–647.

- [16] P. MALLET, C. A. GUÉRIN AND A. SENTENAC, *Maxwell-Garnett mixing rule in the presence of multiple scattering: derivation and accuracy*. Physical Review, B 72 (2005), 14205/1–9.
- [17] V. A. MARCHENKO AND E. YA. KHRUSLOV, *Homogenization of Partial Differential Equations*. Birkhäuser, 2006.
- [18] P. J. M. MONTEIRO, C. Y. PICHOT AND K. BELKEBIR, *Computer tomography of reinforced concrete*. In: Materials Science of Concrete, Chapter 12, American Ceramics Society, 1998.
- [19] G. NGUETSENG AND N. SVANSTEDT,  $\sigma$ -convergence. *Banach Journal of Mathematical Analysis*, 5 (2011), pp. 101–135.
- [20] S. J. ORFANIDIS, *Electromagnetic Waves and Antennas*. Rutgers University, Piscataway (NJ, USA), 2014.
- [21] O. OUCHETTO, S. ZOUHDI, A. BOSSAVIT, G. GRISO AND B. MIARA, *Modeling of 3D periodic multiphase composites by homogenization*. IEEE Transactions on Microwave Theory and Techniques, 54 (2006), pp. 2615–2619.
- [22] N. OZYURT, L. Y. WOO, T. O. MASON AND S. P. SHAH, *Monitoring fiber dispersion in fiber reinforced cementitious materials: comparison of AC-impedance spectroscopy and image analysis*. ACI Materials Journal, 103 (2006), pp. 340–347.
- [23] T. POSPÍŠIL, *On statistical description of random structures*. Engineering Mechanics, 17 (2010), pp. 383–392.
- [24] M. PIEPER AND P. KLEIN, *Application of simple, periodic homogenization techniques to nonlinear heat conduction problems in non-periodic, porous media*. Heat and Mass Transfer, 48 (2012), pp. 291–300.
- [25] L. RIZZUTI AND F. BERNARDINO, *Effects of fibre volume fraction on the compressive and flexural experimental behaviour of SFRC*. Contemporary Engineering Sciences, 7 (2014), pp. 379–390.
- [26] T. ROUBÍČEK. *Nonlinear Partial Differential Equations with Applications*. Birkhäuser, Basel, 2006.
- [27] V. A. RUKAVISHNIKOV AND A. O. MOSOLAPOV, *New numerical method for solving time-harmonic Maxwell equations with strong singularity*. Journal of Computational Physics, 231 (2012), pp. 2438–2448.
- [28] A. H. SIHVOLA AND I. V. LINDELL, *Effective permeability of mixtures*. Progress in Electromagnetics Research, 6 (1992), pp. 153–180.
- [29] D. V. SOULIOTI, N. M. BARKOULA, A. PAPIETIS AND T. E. MATIKAS, *Effects of fibre geometry and volume fraction on the flexural behaviour of steel-fibre reinforced concrete*. International Journal for Experimental Mechanics, 47 (2011), pp. 535–541.
- [30] M. O. STEINHAUSER, *Computational Multiscale Modeling of Fluids and Solids*, Springer, 2008.
- [31] N. SVANSTEDT, *Multiscale stochastic homogenization of convection-diffusion equations*. Applications of Mathematics, 53 (2008), pp. 143–155.
- [32] L. TARTAR, *Quelques remarques sur l'homogenisation*. In: Functional Analysis and Numerical Analysis – Proceedings of the Japan-France Seminar, Japanese Society for Promotion of Science (1978), pp. 136–212.
- [33] M. TUNÁK AND A. LINKA, *Analysis of planar anisotropy of fibre systems by using 2D Fourier transform*. Fibres & Textiles in Eastern Europe, 15 (2007), pp. 86–90.
- [34] R. URBAN, P. FIALA, M. HANZELKA AND J. MIKULKA, *Stochastic models of electrodynamics and numerical models*. 33rd PIERS (Progress In Electromagnetics Research Symposium) in Taipei (China), 2013, pp. 33–37.
- [35] S. VAN DAMME, A. FRANCHOIS, D. DE ZUTTER ND L. TAERWE, *Nondestructive determination of the steel fiber content in concrete slabs with an open-ended coaxial probe*. IEEE Transactions of Geoscience and Remote Sensing, 42 (2004), pp. 2511–2521.
- [36] J. VALA AND M. HORÁK, *Nondestructive identification of engineering properties of metal fibre composites*. 10-th ICNAAM (International Conference of Numerical Analysis and Applied Mathematics) in Kos (Greece), AIP Conference Proceedings, 1479 (2012), pp. 2208–2211.
- [37] J. VALA AND T. GROHOVÁ, *A magnetic approach to the identification of effective characteristics of metal fibre composites used in civil engineering*. Recent advances in integrity, reliability and failure – 4-th International Conference in Funchal (Madeira), 2013, pp. 731–750.
- [38] G. WEIDEMANN, R. STADIE, J. GOEBBELS AND B. HILLEMEIER, *Computer tomography study of fibre reinforced autoclaved aerated concrete*. Materials Testing, 50 (2008), pp. 278–285.
- [39] H.-J. WICHMANN, H. BUDELMANN AND A. HOLST, *Determination of steel fiber dosage and steel fiber orientation in concrete*. In: Nondestructive Testing of Materials and Structures, Springer 2013, pp. 239–245.
- [40] K. W. WHITES AND F. WU, *Effects of particle shape on the effective permittivity of composite materials with measurements for lattices of cubes*. IEEE Transactions on Microwave Theory and Techniques, 50 (2002), pp. 1723–1729.